Isoneutral control of effective diapycnal mixing in numerical ocean models with neutral rotated diffusion tensors

Antoine Hochet[1], Rémi Tailleux[1], David Ferreira[1], and Till Kuhlbrodt[1,2]

[1]Department of Meteorology, University of Reading
[2]National Center for Atmospheric Science

Correspondence to: a.hochet@reading.ac.uk

Abstract. It is well known that in the ocean, there is an infinite number of ways to construct a globally-defined density variable, each possible density variable having a priori its own distinct diapycnal diffusivity. Because no globally-defined density variable can be exactly neutral, numerical ocean models have tended to use rotated diffusion tensors mixing separately in the directions parallel and perpendicular to the local neutral vector, at rates defined by the isoneutral and dianeutral mixing coefficients respectively. To constrain these mixing coefficients from observations, one widely used tool are inverse methods based on Walin-type water masses analyses. Such methods, however, are only able to constrain the diapycnal diffusivity of the globally-defined density variable γ — such as σ_2 for instance — that underlies the inverse method. To use such a method to constrain the dianeutral mixing coefficient therefore requires understanding the inter-relations between the different diapycnal diffusivities. However, this is complicated because the effective diapycnal diffusivity experienced by γ is necessarily partly controlled by isoneutral diffusion owing to the unavoidable misalignment between iso-γ surfaces and the neutral directions. ~~A key challenge in numerical ocean modeling is the parameterisation of the turbulent mixing of heat and salt. Current models mostly use a rotated diffusion tensor based on mixing directions parallel and perpendicular to the local neutral vector. However, there is no density variable that is exactly neutral everywhere because of the coupling between thermobaricity and density-compensated temperature and salinity anomalies. Hence, when using neutral rotated diffusion, the effective diapycnal diffusivity experienced by any possible density variable is necessarily partly controlled by isoneutral diffusion.~~ Here, this effect is quantified by evaluating the effective diapycnal diffusion coefficient ~~for~~ pertaining to five widely used density variables: Jackett and McDougall (1997) γ^n, Lorenz reference state density ρ_{ref} of Saenz et al. (2015), and three potential density variables σ_0, σ_2 and σ_4. Computations are based on the World Ocean Circulation Experiment climatology, assuming either a uniform value for the isoneutral mixing coefficient or spatially varying values inferred from an inverse calculation. Isopycnal mixing contributions to the effective diapycnal mixing yield values consistently larger than 10^{-3} m^2/s in the deep ocean for all density variables, with γ^n suffering the least from the isoneutral control of effective diapycnal mixing, and σ_0 the most. These high values are due to spatially localised large values of non-neutrality, mostly in the deep Southern Ocean. Removing only 5% of these high values on each density surface reduces the effective diapycnal diffusivities to less than 10^{-4} m^2/s. ~~This work highlights~~ The main implication of this work is to highlight the conceptual and practical difficulties of relating the diapycnal mixing diffusivities inferred from global budgets or inverse methods relying on Walin-like water mass analyses to locally defined dianeutral diffusivities. Doing so requires being able to tease out the relative contribution of isoneutral mixing

from the effective diapycnal mixing, and makes it difficult to study diapycnal mixing completely independently of isopycnal mixing. Because it corresponds to a special case of Walin-type water mass analysis, the determination of spurious diapycnal mixing based on monitoring the evolution of the Lorenz reference state may also be affected by the above issues when using a realistic nonlinear equation of state, which has been overlooked so far. ~~Because Lorenz reference density is not exactly neutral, the above issues a priori also pertains to the determination of spurious diapycnal mixing based on monitoring the evolution of Lorenz reference state when using a realistic nonlinear equation of state, which has been overlooked so far.~~ This should be kept in mind when interpreting published estimates of spurious diapycnal mixing, as the present results imply that part of it could in fact be due to isoneutral mixing contamination.

1 Introduction

Tracers in the oceans are stirred and mixed preferentially along isopycnal surfaces Iselin (1939); Montgomery (1940); Solomon (1971). This process is associated with a forward cascade of tracer variance to smaller and smaller scale and ultimately to molecular diffusion. In coarse resolution ocean models where mesoscale eddies are not permitted, this is a subgrid-scale process, which hence needs to be fully parameterised. In such models, it has become commonly accepted, following Redi (1982), to mix potential temperature (alternatively Conservative Temperature) and salinity[1] by means of a rotated diffusion tensor aligned with the local neutral direction. Note that subgrid-scale mixing processes in ocean models include two other important components: dianeutral mixing and eddy-induced advection. ~~as attested for instance by adjoint-model sensitivities, e.g., Forget et al. (2015).~~ Simulations of climate change by means of coupled ocean-atmosphere numerical models are sensitive to parameterisations of oceanic sub-grid scale mixing of heat and salt. It is now well-established that sub-grid scale mixing processes are of key importance for climate change simulations, for they directly control ocean heat uptake, the strength of the Atlantic meridional overturning circulation, and the poleward heat transport e.g., Kuhlbrodt and Gregory (2012); Pradal and Gnanadesikan (2014); Gnanadesikan et al. (2015).

A conceptual difficulty with neutral rotated diffusion tensors, however, is that it is not possible to construct for the ocean a mathematically well defined materially conserved density variable $\gamma(S,\theta)$ whose gradient is parallel to the neutral direction everywhere in the world ocean (McDougall and Jackett, 1988b) (mathematically, the problem arises because the local concept of neutral mixing cannot be extended globally, see Appendix A). This implies that the "effective cross-isopycnal mixing" experienced by a material density variable $\gamma(S,\theta)$, that is, the local diffusive flux of γ through an iso-γ surface (i.e. $\gamma = \mathrm{constant}$) must at least be partly controlled by isoneutral mixing, in a way that depends on the degree of non-neutrality of the density variable considered (Fig. 1). In other words, the diapycnal mixing seen by any isopycnal surface, including the neutral surfaces γ^n of Jackett and McDougall (1997), is "contaminated" by the isoneutral ~~isopycnal~~ mixing. ~~(something which is not always recognized when diagnosing diapycnal mixing in models or observation).~~ Although the issue was raised before in the

---

[1]We assume fixed composition, thus allowing one to treat practical (conductivity) salinity and Absolute Salinity as equivalent, since the two are then linked to each other by a fixed conversion factor. Note that all the arguments could be reformulated using the more recent Conservative Temperature Θ if desired without changing the conclusions.

literature (Lee et al., 2002; McDougall and Jackett, 2005), the idea that the effective diapycnal diffusivity experienced by any mathematically globally defined density variable might be contaminated to some degree by isoneutral mixing and the implied uncertainties are not widely recognized in studies estimating diapycnal mixing, whether it is spurious numerical mixing in models (Griffies et al., 2000; Ilıcak et al., 2012; Lee et al., 2002; Megann, 2018) or inversion/Walin-like estimate of effective

5   mixing in models or observations (Nurser et al., 1999). ~~This potential contamination was noted by~~ (Lee et al., 2002), ~~but they assumed the effect to be second order and made no attempt at quantifying it.~~

A quantification of this effect in terms of diapycnal diffusion is the first aim of this work. We will develop a mathematical framework to estimate the implied diapycnal mixing due to isoneutral mixing on any density surface. Using the observed ocean climatology, we then quantify the contamination of diapycnal diffusion by isoneutral mixing for a series of commonly used

10   density surfaces. We will consider: Jackett and McDougall (1997) γ^n, three potential density variables σ_0, σ_2, σ_4 and the Lorenz reference state density ρ_{ref}. Note that although ω surfaces Klocker et al. (2009) are more neutral than γ^n, no density variable associated with ω-surfaces has been constructed yet, which makes the use of the latter impractical for the present purposes. These density variables have been chosen because they are widely used in the oceanographic community and thus deserve special attention.

15   Our results give for the first time an estimate of the uncertainties associated with diagnosing diapycnal mixing in the presence of isoneutral mixing, ~~for example when employing Walin-like water masse analysis of model outputs or observationor when diagnosing spurious numerical mixing in ocean models~~. The present results suggest the effect might in fact be more important than usually assumed and therefore warranting more attention that it has received. Another motivation for the present study stems from a recent isopycnal justification for the well-known one-dimensional advection/diffusion model for ocean heat

20   uptake, e.g., Huber et al. (2015) in which the diapycnal diffusivity diffusing heat downward is the effective diapycnal diffusivity discussed in the present paper, see https://arxiv.org/abs/1708.02085

The present work and predecessors also raises wider debate on how to measure and interpret measurement of diapycnal mixing as it is not easily separated from isoneutral mixing and this absence of separation depends on the choice of density surface used for the diagnostic. On a related level, the mathematical framework we use below clearly reveal that, for a given

25   turbulent flux, an infinite number of projections, and thus of iso/diapycnal diffusion coefficients, each associated to a choice of density surface, are possible.

Section 2 presents the theoretical framework used for defining effective diffusivities for each variable. We also discuss how our framework relates to similar concepts and approaches previously published. Section 3 present estimates of the diapycnal diffusion contamination due to isoneutral mixing for the above mentioned five density variables. Sensitivity of the results to

30   the choice of isoneutral mixing and location is also discussed. In section 4, we discuss the larger implications of our findings and the related issue of defining/measuring/comparing mixing coefficients. Finally, Section 5 summarizes and discusses the results.

2 Method

2.1 Effective diffusivity

Thermodynamic properties in numerical ocean models are commonly formulated in terms of θ and S, whose evolution equations can in general be expressed as:

$$\frac{D_{\text{res}}\theta}{Dt} = \nabla \cdot (\mathbf{K}\nabla\theta) + f_\theta, \qquad \frac{D_{\text{res}}S}{Dt} = \nabla \cdot (\mathbf{K}\nabla S) + f_S, \tag{1}$$

where $\mathbf{K} = K_i(\mathbf{I} - \mathbf{d}\cdot\mathbf{d}^T) + K_d\mathbf{d}\cdot\mathbf{d}^T$ is Redi (1982)'s neutral rotated diffusion tensor (with K_i and K_d being the isoneutral and dianeutral turbulent mixing coefficients respectively, $\mathbf{d} = \mathbf{N}/|\mathbf{N}|$ the locally-defined normalised neutral vector), f_S, f_θ respectively the forcing terms for salinity and potential temperature and $D_{\text{res}}/Dt = \partial/\partial t + (\mathbf{v} + \mathbf{v}^\star)\cdot\nabla$ the advection by the residual velocity (the sum of the Eulerian velocity and the mesoscale eddy-induced velocity). A common parameterisation for $\mathbf{v}^\star$ is that of Gent and McWilliams (1990), see also Griffies (2004), but note that the following arguments are independent of the precise form of $\mathbf{v}^\star$. Note here that K_i and K_d are implicitly defined in terms of the orthogonal projections of the turbulent heat and salt fluxes on the isoneutral and dianeutral directions; for an alternative and more recent definition of K_i and K_d aimed at making dianeutral mixing appear to be isotropic, see McDougall et al. (2014). For the sake of clarity, the directions parallel and perpendicular to the local neutral tangent planes are referred to as 'dianeutral' and 'isoneutral' respectively, the terms 'diapycnal' and 'isopycnal' being used when isopycnal surfaces are defined in terms of a material density variable $\gamma(S,\theta) = \text{constant}$. The evolution equation of any material density variable $\gamma(S,\theta)$ is:

$$\frac{D_{res}\gamma}{Dt} = \nabla \cdot (\mathbf{K}\nabla\gamma) - \underbrace{\left(\gamma_{\theta\theta}\nabla\theta^T\mathbf{K}\nabla\theta + 2\gamma_{S\theta}\nabla S^T\mathbf{K}\nabla\theta + \gamma_{SS}\nabla S^T\mathbf{K}\nabla S\right)}_{NL}. \tag{2}$$

Unless $\gamma(S,\theta)$ is a linear function of S and θ, its evolution equation will in general contain non vanishing nonlinear terms (denoted NL in Eq. (2)) related to cabelling and thermobaricity, e.g., McDougall (1987); Klocker and McDougall (2010); Urakawa et al. (2013). The diffusive flux of γ is:

$$F_{\text{diff}}^\gamma = -\mathbf{K}\nabla\gamma = \underbrace{-K_i(\nabla\gamma - (\nabla\gamma\cdot\mathbf{d})\mathbf{d})}_{F_{\text{diff}}^i} \underbrace{-K_d(\nabla\gamma\cdot\mathbf{d})\mathbf{d}}_{F_{\text{diff}}^d}, \tag{3}$$

where F_{diff}^i and F_{diff}^d are respectively the diffusive flux of γ in the isoneutral and dianeutral direction. For clarity, figure 1 shows a schematic of the neutral plane, of the $\gamma = \text{const.}$ plane, of the $\nabla\gamma$ and neutral direction and of F_{diff}^i and F_{diff}^d.

We define the effective diffusive flux of γ as the integral of the diffusive flux across the isopycnal surface $\gamma(\mathbf{x},t) = \text{constant}$, viz.,

$$F_{\text{eff}} = -\int_{\gamma=\text{const}} \mathbf{K}\nabla\gamma\cdot\mathbf{n}\,\mathrm{d}S \tag{4}$$
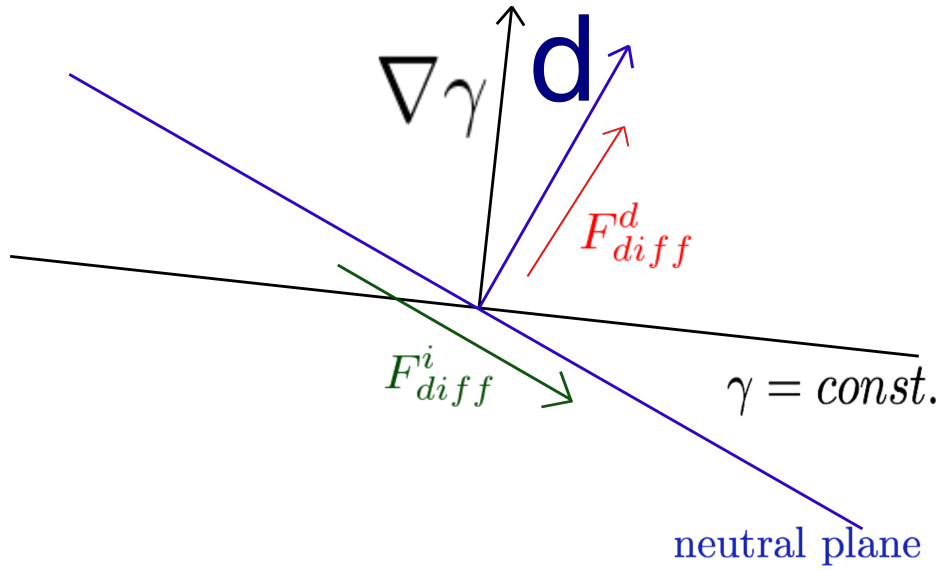
Figure 1. Schematic showing the neutral plane and neutral direction $\mathbf{d}$ in blue, the $\gamma = \text{const.}$ plane and $\nabla\gamma$ direction in black and the projection of the diffusive flux of γ in the isoneutral (F_{diff}^i) and dianeutral (F_{diff}^d) direction.

where $\mathbf{n} = \frac{\nabla\gamma}{|\nabla\gamma|}$ is the unit local normal vector to the γ surface. Now, it is easily established after some straightforward algebra that:

$$
\begin{aligned}
K\nabla\gamma \cdot \mathbf{n} &= [K_i(\nabla\gamma - (\nabla\gamma \cdot \mathbf{d})\mathbf{d}) + K_d(\nabla\gamma \cdot \mathbf{d})\mathbf{d}] \cdot \frac{\nabla\gamma}{|\nabla\gamma|} \\
&= \left[K_i \left(|\nabla\gamma|^2 - (\nabla\gamma \cdot \mathbf{d})^2 \right) + K_d(\nabla\gamma \cdot \mathbf{d})^2 \right] / |\nabla\gamma| \\
&= |\nabla\gamma| \left[K_i \sin^2(\nabla\gamma, \mathbf{d}) + K_d \cos^2(\nabla\gamma, \mathbf{d}) \right].
\end{aligned}
\tag{5}
$$

Eq. (5) establishes that the locally defined effective diapycnal diffusivity experienced by the density variable γ is affected by both isoneutral and dianeutral mixing, the contribution from isoneutral mixing being akin to a Veronis-like effect, as discussed in Tailleux (2016). Because we are primarily interested in the latter effect, we shall discard the effect of dianeutral mixing on the effective diapycnal diffusivity of γ and hence assume $K_d = 0$ in the rest of the paper. As a result, the expression for the effective diapycanl diffusive flux of γ due to isoneutral mixing becomes:

$$
F_{\text{eff}} = - \int\limits_{\gamma=\text{const}} |\nabla\gamma| K_i \sin^2(\nabla\gamma, \mathbf{d}) \mathrm{d}S.
\tag{6}
$$

Note that the integrand of (6) is mathematically equivalent to what McDougall and Jackett (2005) refer to as "fictitious diapycnal mixing". However, here the integrand is integrated on γ surfaces and then used to calculate an effective diffusivity coefficient which is easier to interpret than a collection of local values of the $(\nabla\gamma, \mathbf{d})$ angle.

2.2 Reference Profile

In order to construct an effective turbulent diffusivity K_{eff} associated with the effective diffusivity flux F_{eff}, we need to define an appropriate mean gradient for the density variable γ. This is done by constructing a reference profile for γ, as explained in the next paragraph.

Let $z_r(\gamma, t)$ be the reference profile for the particular material density $\gamma(S, \theta)$ (which can always be written as a function of space $\mathbf{x}$ and time t as $\gamma^*(\mathbf{x}, t) = \gamma(S, \theta)$), constructed to be the implicit solution of the following problem:

$$\int_{V(z_r)} \mathrm{d}V = \int_{V(\gamma, t)} dV = \int_{z_r(\gamma, t)}^{0} A(z)dz, \tag{7}$$

where $A(z)$ is the depth-dependent area of the ocean at depth z, and $V(\gamma, t)$ the volume of water for all parcels with density γ_0 such that $\gamma_0 \leq \gamma$. The knowledge of the reference profile allows one to regard the volume $V(\gamma, t)$ of water masses with density lower than γ as a function of z_r only as $V(\gamma, t) = V(z_r(\gamma, t))$. Physically, Eq. (7) defines the reference depth $z_r(\gamma, t)$ at which the volume of water with density lower than γ is equal to the volume of water comprised between the ocean surface and z_r; this definition is equivalent to that used by Winters and D'Asaro (1996) (see also Griffies et al. (2000), Saenz et al. (2015)) to construct the Lorenz reference state, but generalised here to the case of an arbitrary materially conserved density variable $\gamma(S, \theta)$. Once $z_r(\gamma, t)$ is constructed, it can be inverted to define in turn the reference profile $\gamma_r(z_r, t)$ as $\gamma_r(z_r(\mathbf{x}, t), t) = \gamma^*(\mathbf{x}, t)$. As a result, we can always write a relation such as:

$$\nabla \gamma = \frac{\partial \gamma_r}{\partial z_r} \nabla z_r \tag{8}$$

However, the choice of $\gamma(S, \theta)$ influences the local projection of the iso-dianeutral diffusion on the γ gradient and thus the effective diapycnal coefficient. We now define the effective diffusivity K_{eff}. Using (8) in (6), we get:

$$F_{\text{eff}} = -\int_{\gamma=\text{const}} |\nabla \gamma| K_i \sin^2(\nabla \gamma, \mathbf{d}) dS = \frac{\partial \gamma_r}{\partial z_r} \int_{z_r=\text{const}} |\nabla z_r| K_i \sin^2(\nabla z_r, \mathbf{d}) \mathrm{d}S = A(z_r) K_{\text{eff}} \frac{\partial \gamma_r}{\partial z_r}, \tag{9}$$

where we have used $|\nabla \gamma| = -\frac{\partial \gamma_r}{\partial z_r} |\nabla z_r|$ (because $\frac{\partial \gamma_r}{\partial z_r} < 0$). K_{eff} is defined as follows:

$$K_{\text{eff}}(z_r) = \frac{\int_{z_r=\text{const}} K_i |\nabla z_r| \sin^2(\nabla z_r, \mathbf{d}) \mathrm{d}S}{A(z_r)}, \tag{10}$$

which is independent of the gradient of γ_r in the reference space. A detail description of the steps required to obtain K_{eff} is provided in appendix B. Eq. (10) is one of the key results of this study.

Note that K_{eff} is not the surface average of the local mixing coefficient across $\gamma = \text{const.}$ surfaces but rather the mixing coefficient linked to the time variation of γ_r as can be seen from the following equation (proof shown in appendix C):

$$\frac{\partial \gamma_r}{\partial t} = \frac{1}{A(z_r)} \frac{\partial}{\partial z_r} \left(A(z_r) K_{\text{eff}}(z_r) \frac{\partial \gamma_r}{\partial z_r} \right) + \text{NL} + \text{F}, \tag{11}$$

where NL is a term due to the non linearity of $\gamma(S, \theta)$ and F is a term due to the heat and haline fluxes at the ocean surface. Note that in Speer (1997) and in Lumpkin and Speer (2007), the effective diffusivity is defined as the integral of the local

diapycnal flux on a γ surface over the integral of the local gradient of γ on the same γ surface i.e.:

$$K_{\text{eff}}^{\text{speer}} = \frac{\int_{z_r=\text{const}} K\nabla\gamma \cdot \mathbf{n}dS}{\int_{z_r=\text{const}} \nabla\gamma \cdot \mathbf{n}dS}, \tag{12}$$

this is different from our formulation because of the different mean gradient formulation. The relationship between the K_{eff} described in this article (a generalization of Winters and D'Asaro (1996)'s formulation) and $K_{\text{eff}}^{\text{speer}}$ is, from formula (10) and (12):

$$K_{\text{eff}} = K_{\text{eff}}^{\text{speer}} \left(\frac{\int_{z_r=\text{const}} |\nabla z_r|dS}{A(z_r)} \right). \tag{13}$$

We have checked that for all the density variables under consideration here the quantity between brakets in (13) is smaller than 1 so that K_{eff} can be seen as a lower bound of $K_{\text{eff}}^{\text{speer}}$. In Lee et al. (2002), the effective diapycnal coefficient formulation is similar to that of Speer (1997) except that the mean gradient is approximated by an average of the vertical gradient of γ on a γ surface (which is valid as long as the γ slope is small).

3   Isoneutrally-controlled effective diapycnal diffusivities for σ_0, σ_2, σ_4, γ^n and ρ_{ref}

In this section we seek to estimate the effective diffusivity (10) derived in the previous section for five different density variables: σ_0, σ_2, σ_4, the Jackett and McDougall (1997)'s γ^n and the Lorenz reference density ρ_{ref} obtained with Saenz et al. (2015) method. All the calculations of this section are performed with annual mean potential temperature and salinity data from the World Ocean Circulation Experiment (Gouretski and Koltermann, 2004). Since γ^n is not well defined North of $60°$N, the latter region was excluded from our analysis for all five density variables. Since eddies mix the fluid horizontally in the mixed layer rather than perpendicular to the neutral vector, we also restrict our calculation to the ocean below the mixed layer. Here, the depth of the mixed layer is taken from the de Boyer Montégut database (de Boyer Montégut et al., 2004). The reference density for each of the five variables is shown on Fig. 2. As expected, the range of values taken by the reference density of the three potential density variables increases with the reference pressure. γ^n has a reference density similar to that of σ_0 with a slightly smaller gradient in the reference space. ρ_{ref} has a gradient much larger than all other density variables. It crosses σ_0 at the surface, σ_2 around -2000 meters and σ_4 around -4000 meters. This is due to the fact that the volume above the surface $\sigma_p(\theta,S) = \sigma_p^r(Z)$ is by definition the same as the volume above $\rho(\theta,S,p) = \rho_{ref}(Z)$ where $p = -Z\rho_0 g$ is the reference pressure linked to the reference depth Z, σ_p^r is the reference density linked to σ_p.

Figure 3 shows the histogram of the decimal logarithm of the squared sine of the angle between $\nabla\gamma$ and $\mathbf{d}$ (calculated using Eq. (B1) in appendix B), $\log_{10}[\sin(\nabla\gamma, \mathbf{d})]$ [missing square?]. This plot is similar to that discussed by McDougall and Jackett (2005) in their discussion of fictitious diapycnal mixing.

ρ_{ref}, σ_2 and σ_4 give similar angles with most of their values slightly larger than 10^{-5}. γ^n gives the smallest angles among the variables under consideration here with most of its values smaller than 10^{-5} while σ_0 gives the largest with a large number of points with values larger than 10^{-4}. All together, these observations could suggest that the effective diffusivity of γ^n should
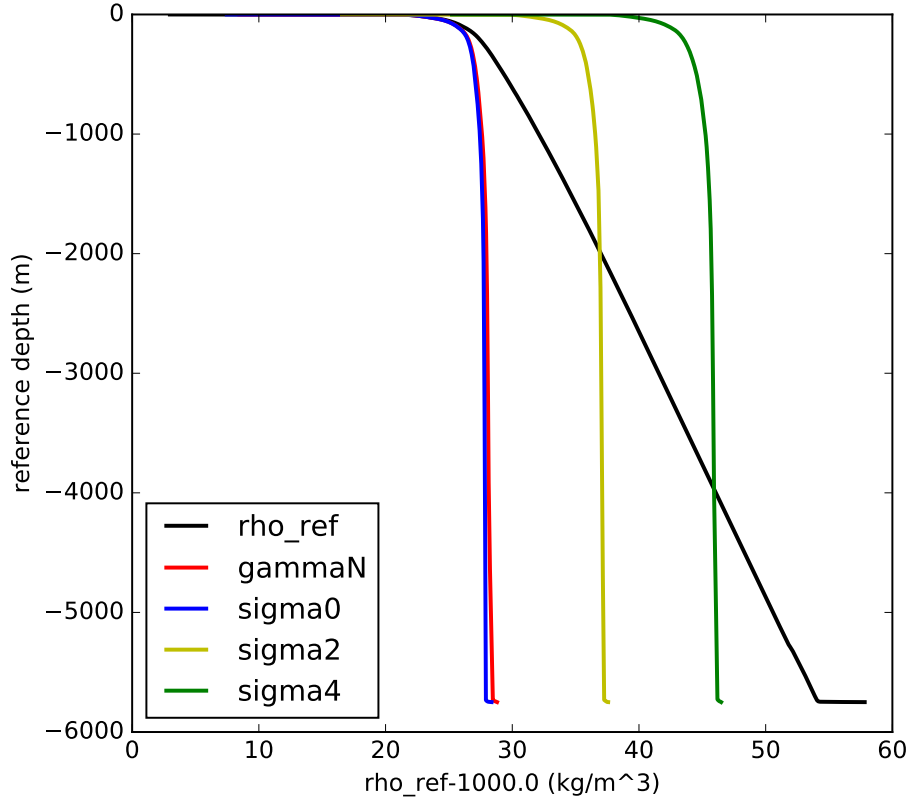
Figure 2. Reference density for ρ_{ref} (black) γ^n (red), σ_0 (blue), σ_2 (yellow) and σ_4 (green) as a function of the reference depth.

be the smallest overall, that the effective diffusivity of ρ_{ref} should be of the same order as that for σ_2 and σ_4, and that the effective diffusivity for σ_0 should be the largest of all. It is however hard to predict the values of the effective diffusivity coefficient for each density variable from figure 3 only since the small number of point with very large angle values (hardly visible on figure 3) could dominate the large number of points with small angles and since the spatial variability of the isoneutral mixing coefficient could correlates with the spatial variability of the angle. We thus calculate the effective diffusivity coefficient using these angles values for each density variable.

Figure 4 shows the decimal logarithm of the effective diffusivity K_{eff} for the five variables as a function of the reference depth under two possible choices of K_i:

The first case (A, figure 4) assumes a constant isoneutral coefficient: $K_i = 1000$ m^2/s. Under this assumption, K_{eff} for every density variables increases on average with the reference depth from values between 10^{-12} and 10^{-8} m^2/s close to surface reference depth to values between 10^{-6} and 0 m^2/s at the deepest reference depths. This increase reflects that the
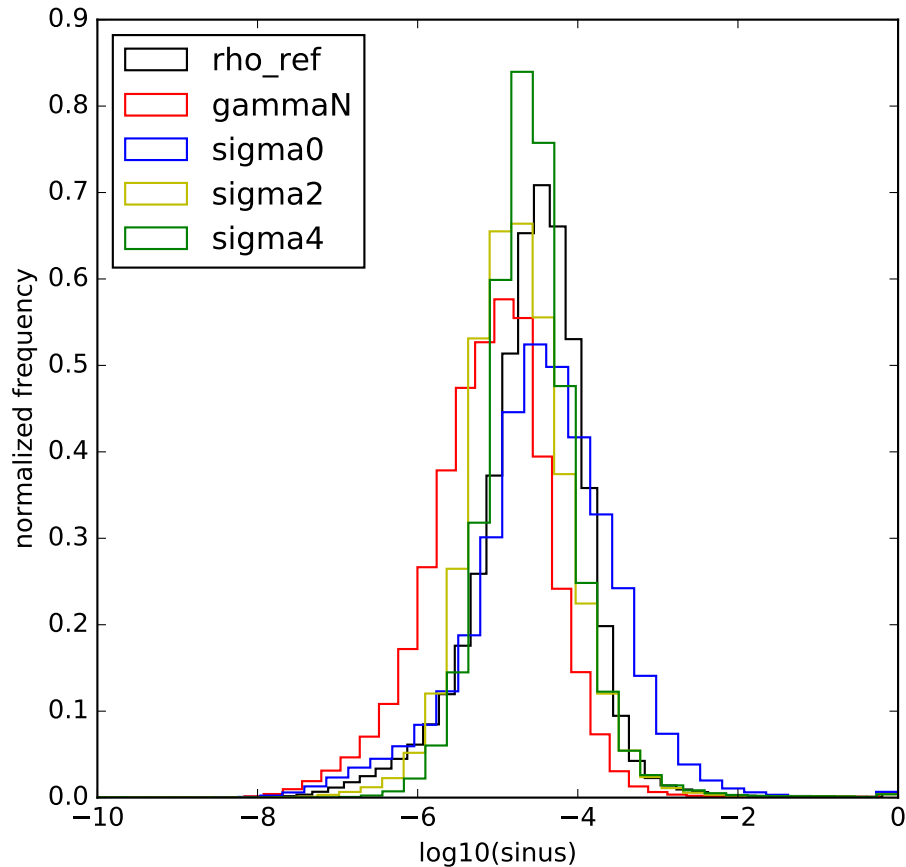
Figure 3. Histogram of the decimal logarithm of the squared sine between the gradient of γ and the neutral vector **d** weighted by the volume of each point. $\log_{10}\left(\sin\left(\nabla\gamma, \mathbf{d}\right)\right)$ [missing square?] for ρ_{ref} (black), γ^n (red), σ_0 (blue), σ_2 (yellow) and σ_4 (green).

largest discrepancy between the neutral vector and the gradients of the 5 density variables is generally located in the Antarctic Circumpolar Current (ACC) where the highest densities, and thus deepest reference depths, outcrop (see below).

K_{eff} for γ^n and σ_0 are similar between 0 and 800 m depth with values ranging from 10^{-8} m^2/s at the surface to 10^{-6} m^2/s at -800 meters. σ_2, σ_4 and ρ_{ref} give values up to 100 larger on the same depth range. Between 800 and 4000 m depth, γ^n gives

5   the smallest K_{eff} which is slowly increasing from 10^{-6} to 10^{-5} m^2/s as the depth decreases. On the same depths, ρ_{ref}, σ_0, σ_2 and σ_4 gives values at least 10 times larger (up to 1000 times larger for σ_0 below -2000 m). Below 4000 m depth, all density variables have a K_{eff} larger than 10^{-4} m^2/s (note that 10^{-4} m^2/s is the widely cited Munk (1966) and Munk and Wunsch (1998)'s canonical estimate of diapycnal mixing inferred from the global heat and mechanical energy budgets.) At the deepest levels, under -5000 meters, σ_0 and ρ_{ref} have a smaller K_{eff} than γ^n suggesting that their local gradients are very nearly aligned

10 with the neutral vector at these deep reference depths.
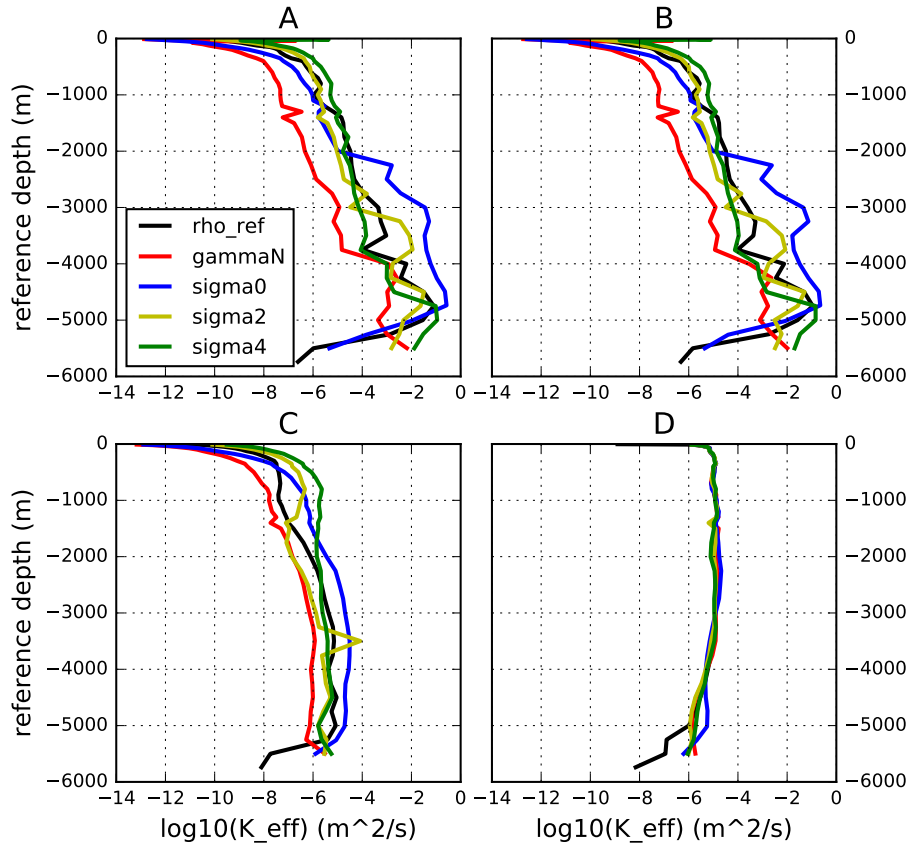
Figure 4. $\log_{10}$ of the effective diapycnal diffusivity coefficient K_{eff} as a function of the reference depth (meters) (and as defined by equation (10)) for ρ_{ref} (black), γ^n (red), σ_0 (blue), σ_2 (yellow) and σ_4 (green). Panels A,B and C correspond to a K_{eff} calculated with different isoneutral diffusivity coefficient. A: $K_{iso} = 1000$ m^2/s, B: variable isoneutral diffusivity coefficient given by Forget et al. (2015). C: same as B but without 5% of the largest angles. Bottom right, D: $\log_{10} K_{\mathrm{eff}}$ calculated from a variable dianeutral diffusivity coefficient given by the inverse calculation of Forget et al. (2015)

.

The second case (B, figure 4) assumes a spatially variable isoneutral coefficient given by the inverse calculation of Forget et al. (2015), which gives a three dimensional distribution of K_i at about $1°$ resolution for the global ocean. This database contains values ranging from 9000 m^2/s (in the Atlantic deep water formation zone at the surface, in western boundary currents and ACC) to values close to 0 (in the deep pelagic ocean). The estimated K_{eff} for this choice are very close to those obtained under the previous assumption of constant diffusivity for all variables, showing the small sensitivity of our results to spatial variations of isoneutral diffusion, which is further discussed below.

To investigate the importance of the localised large departure from neutrality in the construction of K_{eff}, we removed 5% of the largest non-neutral values of the angle for each reference surface (figure 4, case C). Without 5% of the largest values, K_{eff} is much smaller than the previous one for every density variables with values everywhere smaller than 10^{-4} m^2/s. As before, the effective diffusivity increases rapidly close to the surface and then more slowly below -1000 meters (except at a few depth for σ_2, σ_4 and at deep reference depth for ρ_{ref} and σ_0) with the reference depth for all density variables. γ^n gives the smallest values for almost all reference depths, with values from 10^{-10} m^2/s close to the surface of the reference space to 10^{-6} m^2/s at the deepest levels. σ_2 gives the second smallest values for reference depths smaller than -1500 meters but is overtaken by σ_0 and ρ_{ref} at larger depths. ρ_{ref},σ_0, σ_2 and σ_4 all give effective diffusivities of the order or larger than 10^{-5} m^2/s at some depth below -2000 meters.

This calculation shows that the isoneutral contribution to effective diapycnal mixing is very localised spatially with 5% of each surface accounting for most of the effective diffusivity for all the density variables under consideration here. However, even without this top 5%, K_{eff} remains close or above 10^{-5} m^2/s for all variables except γ^n. Coming back to the similarity between panels A and B, the location of the top 5% values are correlated with local K_i values (from Forget et al. (2015) database) around 1000 m^2/s which therefore explain the lack of sensitivity of our results on the choice of K_i between A and B.

Panel D shows K_{eff} calculated using a dianeutral mixing coefficient given by Forget et al. (2015) inverse calculation assuming no isoneutral mixing. The formula for this calculation is obtained by replacing the sine by a cosine and K_i by K_d in formula (10) following formula (5), i.e. :

$$K_{\text{eff}}(z_r) = \frac{\int_{z_r=\text{const}} K_d |\nabla z_r| \cos^2(\nabla z_r, \mathbf{d}) \mathrm{d}S}{A(z_r)}. \tag{14}$$

K_{eff} values are smaller or close to 10^{-5} m^2/s at all reference depths for all density variables. For reference depth deeper than 1000 meters, these values are much smaller than the effective diffusivity estimated from the isoneutral mixing coefficient as shown on panel A or B. Without the 5% of the largest values on each density surface, K_{eff} estimated from variable K_i (panel C) is smaller than the one estimated from variable K_d for all density variables above 1000 meters. The exception is γ^n which gives K_{eff} estimated from K_i approximately 10 times smaller than K_{eff} from K_d at all reference depths below 1000 m. Note that the values obtained from the dianeutral coefficient are much less sensitive to the choice of density variable than the values obtained from the isoneutral mixing coefficient, since for small angles, $\cos^2(\nabla z_r, \mathbf{d}) \approx 1 - (\nabla z_r, \mathbf{d})^2$ depends on the angle only at second order. ~~This is because of the 7 order of magnitude difference between K_d and K_i which makes the K_{eff} estimated from the isoneutral coefficient much more sensitive to the angle between the neutral vector and the local gradient of the density variable under consideration.~~ As illustrated in Fig. 5, the largest angles between the neutral vector and the gradient of the density variable are found mostly in the ACC at all depth for ρ_{ref} and γ^n and everywhere at depth for σ_0, suggesting that, in this region, all the density variables studied above introduce significant biases in the estimation of diapycnal mixing.
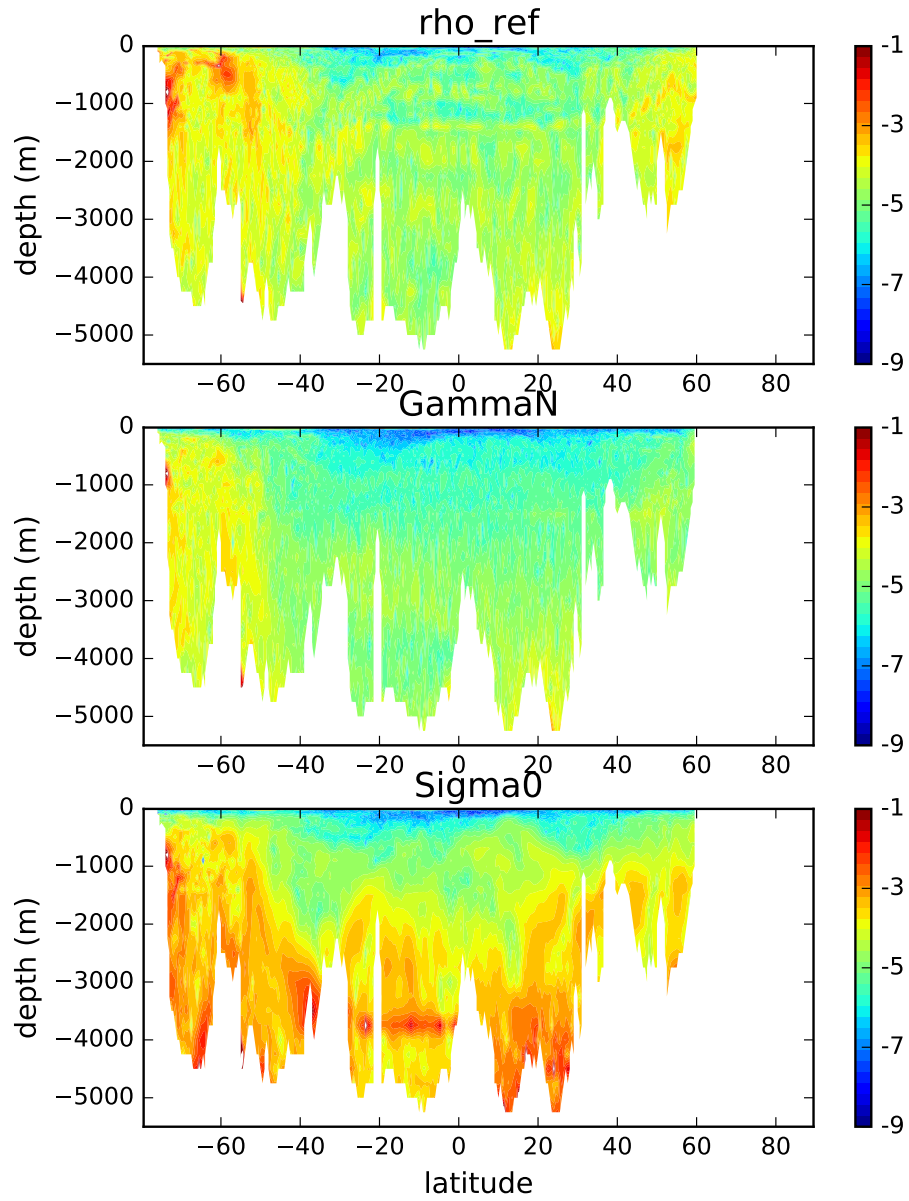
Figure 5. Decimal logarithm of the sine between the neutral vector and the gradient of ρ_{ref} (top), γ^n (middle) and σ_0 (bottom) as a function of latitude and depth at 30^oW (in the Atlantic).

4 Conclusions

Mixing of heat and salt in numerical ocean models is commonly parameterised by means of a neutral rotated diffusion tensor using dianeutral and isoneutral mixing coefficients K_d and K_i relating to density surfaces that are only defined locally ~~that do not a priori relate to the mixing of any globally-defined density variable~~. In contrast, inverse methods based on Walin-type water masses analyses produce observationally constrained diapycnal diffusivities K_γ for the globally-defined density variable γ underlying the isopycnal analysis. Since inverse methods give us information about K_γ, while what we need in numerical ocean models is K_d, our ability to use Walin-type inverse approaches to constrain neutral rotated diffusion tensors therefore depends on our ability to understand how the various diffusivities K_γ and K_d are inter-related.

In this paper, we have presented a new framework for assessing the contribution of isoneutral diffusion to the effective diapycnal mixing coefficient K_{eff} for five different density variables, chosen for their widespread use in the oceanographic community, namely $\gamma^n, \rho_{ref}, \sigma_0, \sigma_2, \sigma_4$. Our results reveal that the contribution of isoneutral mixing to the effective diapycnal mixing experienced by each density variable can be as large as 10^{-4} m^2 s^{-1} and up to 0.1 m^2 s^{-1} for reference depths deeper than 2000 meters. These values are typically 10 to 100 times larger below -1000m and up to 1000 times larger below -4000 meters than estimations for the effective diapycnal mixing due to the dianeutral mixing alone (which are around or below 10^{-5} m^2 s^{-1}). As expected, γ^n, constructed to be as neutral as practically feasible, is the least affected by isoneutral diffusion of all density variables considered. Nevertheless, it still appears to experience values larger than 10^{-4} m^2 s^{-1} for reference depths below -4000 meters. These values are 10 to 100 times larger than the corresponding effective mixing due to the direct effect of a (variable) dianeutral mixing coefficient. Note that an added difficulty pertaining to the use of γ^n stems from its non-material character. As a result, the validity of defining an effective diapycnal diffusivity for γ^n using the present approach depends on such non-material effects to be small, or at least much smaller than the contribution from isopycnal diffusion discussed here, which is difficult to evaluate.

Our results thus suggest that the potential contamination due to isoneutral mixing should always be assessed for any inference of diapycnal mixing based on the use of any density variable $\gamma(S, \theta)$ in Walin-like water mass analysis for instance. In agreement with previous studies (e.g. McDougall and Jackett, 2005), the regions of large discrepancy between the neutral vector and the gradient of each surface are ~~very~~ localised in space, and mainly confined to the deep Southern Ocean. However, while representing a very small amount of volume of the ocean, these discrepancies are important in setting the effective diffusivity values. Indeed, without 5% of the largest angle values between the neutral vector and the local γ gradient, all variables give an effective diapycnal mixing smaller than 10^{-4} m^2/s. Moreover, the estimated values are everywhere comparable to or smaller than the effective mixing estimated from dianeutral mixing only. Note that, even after removal of the largest angles, isoneutral and dianeutral mixing equally contribute to the effective diapycnal mixing. In the context of inverse methods, this still represent a potential uncertainty of up to a factor two on the estimation of diapycnal mixing due to the contamination by isoneutral mixing. The concentration of discrepancies is even stronger for γ^n since the effective diffusivity coefficient after the removal of the 5% of the largest values decreases below 10^{-6} m^2/s. This is a contamination of only 10% for typical diapycnal

mixing values of 10^{-5} m^2 s^{-1} found in the thermocline and abyssal plains (Ledwell et al., 1998) and much less for enhanced mixing values found above rough topography (Polzin et al., 1997).

Overall, the K_{eff} profiles for each density variables become similar without the 5% suggesting that the choice of the density variable is less important when the Southern ocean is not taken into account. However, when no part of the ocean is removed (as it is the case in Walin (1982) type calculation for instance), the effective diffusivities found in this article are very sensitive to the density variable under consideration. This is at odd with the results of Megann (2018) and could suggest that their effective diffusivities are mainly driven by spurious numerical mixing.

Our results show that the evaluation of effective diapycnal mixing using a sorting algorithm of density (e.g. Griffies et al., 2000; Hill et al., 2012; Ilıcak et al., 2012), which amounts to diagnosing the diapycnal flux through ρ_{ref}, is likely to be significantly contaminated by isoneutral diffusion owing to the large departures from neutrality of ρ_{ref} in the polar regions if a nonlinear equation of state is used (which is not the case in the above cited studies). Note that this is a distinct effect from the density sinks and sources due to the non-linear equation of state influencing the time variation of the reference density (see equation (11)) which are also a source of contamination of the diapycnal flux from the isoneutral diffusion when using sorting algorithm. It follows that diagnosing the spurious diapycnal mixing resulting from numerical advection schemes for a nonlinear equation of state remains an outstanding challenge, and that progress on this topic must take into account the theoretical considerations developed here.

This work advocates for the construction of a density function $\gamma(\theta, S)$ that would minimizes the influence of isoneutral mixing on the effective diapycnal diffusivity coefficient. So far, the best material density variable is a function of Lorenz reference density, as shown by Tailleux (2016a), but as discussed by Tailleux (2016), it appears theoretically possible to construct an even more neutral one. Whether Klocker et al. (2009) can be used for global inversions is unclear, because its improved neutrality might be achieved at the expenses of materiality, which remains to be quantified.

Appendix A

A conceptual difficulty with neutral rotated diffusion tensors is that it is not possible to construct for the ocean a mathematically well defined materially conserved variable $\gamma(S, \theta)$ allowing to write $\mathbf{N} = C_0 \nabla \gamma$, with C_0 some integrating factor. In the spatial domain, this can be attributed mathematically to the non-zero helicity of $\mathbf{N}$ (see McDougall and Jackett (1988a)). More instructive and illuminating, however, is to prove the result directly in thermohaline space. To that end, let us assume that such a variable $\gamma = \gamma(S, \theta)$ exists, and show that it leads to a contradiction. To that end, let us perform a change of variables from (S, θ) space to (γ, θ) space, similarly as in Tailleux (2016). Let us denote by $J = \partial(\gamma, \theta)/\partial(S, \theta)$ the Jacobian of the transformation. It is easy to see that $J = \partial \gamma/\partial S$, which we assume to be non-zero, so that the transformation is invertible. This makes it possible to regard $S = \hat{S}(\gamma, \theta)$ as a function of γ and θ. Likewise, we can define $\rho = \rho(S, \theta) = \rho(\hat{S}(\gamma, S), \theta) = \hat{\rho}(\gamma, S)$, where the hat notation refers to the variables viewed as functions of γ and θ instead of S and θ. As a result, the neutral vector

can be equivalently written as:

$$\mathbf{N} = -\frac{g}{\rho}\left(\frac{\partial\rho}{\partial S}\nabla S + \frac{\partial\rho}{\partial\theta}\nabla\theta\right) = -\frac{g}{\rho}\left(\frac{\partial\hat{\rho}}{\partial\gamma}\nabla\gamma + \frac{\partial\hat{\rho}}{\partial\theta}\nabla\theta\right). \tag{A1}$$

In order for $\mathbf{N}$ to align with $\nabla\gamma$, one would need the quantity $\partial\hat{\rho}/\partial\theta$ to vanish. An expression for $\partial\hat{\rho}/\partial\theta$ can be obtained using the following series of identities

$$\frac{\partial\hat{\rho}}{\partial\theta} = \frac{\partial(\hat{\rho},\gamma)}{\partial(\theta,\gamma)} = \frac{\partial(\rho,\gamma)}{\partial(S,\theta)}\frac{\partial(S,\theta)}{\partial(\theta,\gamma)} = \frac{1}{J}\frac{\partial(\gamma,\rho)}{\partial(S,\theta)} \tag{A2}$$

where we used the usual properties of Jacobian operators, including composition and anti-symmetry. Eq. (A2) shows that for $\partial\hat{\rho}/\partial\theta = J^{-1}\partial(\gamma,\rho)/\partial(S,\theta)$ to be zero would require ρ to be a function of $\gamma(S,\theta)$ alone, but this cannot be true, because ρ also depends on pressure.

Appendix B: Calculation of K_{eff}

The following steps describe in detail the calculation of the effective diffusivity coefficient for a given $\gamma(S,\theta)$:

1. the reference depth $z_r(S,\theta)$ is calculated following formula (7), its gradient $|\nabla z_r|$ is then computed everywhere;

2. the neutral vector is calculated as the gradient of the locally referenced potential density;

3. the sinus of the angle between ∇z_r and $\mathbf{d}$, $\sin(\nabla z_r, \mathbf{d})$, is calculated using the cross product between ∇z_r and $\mathbf{d}$:

$$|\sin(\nabla z_r, \mathbf{d})| = \frac{|\nabla\mathbf{z_r} \times \mathbf{d}|}{|\nabla\mathbf{z_r}|} \tag{B1}$$

where $\times$ is the cross product and $\mathbf{d}$ the normalised neutral vector $\mathbf{d} = \mathbf{N}/|\mathbf{N}|$;

4. the product $K_i|\nabla z_r|\sin^2(\nabla z_r)$ is interpolated and integrated on $z_r(S,\theta) = \mathrm{const.}$ surfaces;

5. K_{eff} is then equal to the integral obtained at the previous step divided by the area of the ocean at depth z_r i.e. $A(z_r)$.

Appendix C: equation (11)

The evolution equation for γ is:

$$\frac{d\gamma}{dt} = \frac{\partial\gamma}{\partial\theta}\frac{d\theta}{dt} + \frac{\partial\gamma}{\partial S}\frac{dS}{dt} = \frac{\partial\gamma}{\partial\theta}\nabla\left(K\nabla\theta\right) + \frac{\partial\gamma}{\partial S}\nabla\left(K\nabla S\right) + \frac{\partial\gamma}{\partial\theta}f_\theta + \frac{\partial\gamma}{\partial S}f_S \tag{C1}$$

$$= \nabla\left(K\nabla\gamma\right) - K\nabla\theta\cdot\nabla\left(\frac{\partial\gamma}{\partial\theta}\right) - K\nabla S\cdot\nabla\left(\frac{\partial\gamma}{\partial S}\right) + f_\gamma \tag{C2}$$

where f_θ, f_S are the surface heat and haline fluxes and where $f_\gamma = \frac{\partial \gamma}{\partial \theta} f_\theta + \frac{\partial \gamma}{\partial S} f_S$. Then let $z_r(X,t)$ be the reference level of γ defined by equation (7) so that γ can now be written: $\gamma(S,\theta) = \gamma_r(z_r,t)$. Then integrating (C2) on a volume $V(z_r)$ defined by water parcels of reference level larger than or equal to z_r gives:

$$\int\limits_{V(z_r)} \frac{\partial \gamma}{\partial t} dV + \gamma_r(z_r,t) \int\limits_{z_r=\text{const}} \mathbf{u} \cdot \mathbf{n} dS = \int\limits_{z_r=\text{const}} K\nabla\gamma \cdot \mathbf{n} dS - \int\limits_{V(z_r)} K\nabla\theta \cdot \nabla(\frac{\partial\gamma}{\partial\theta}) + K\nabla S \cdot \nabla(\frac{\partial\gamma}{\partial S}) dV + \int\limits_{V(z_r)} f_\gamma dV \quad \text{(C3)}$$

5   where $z_r = \text{const}$ refers to the constant z_r surface. $\mathbf{n} = \frac{\nabla\gamma}{|\nabla\gamma|} = -\frac{\nabla z_r}{|\nabla z_r|}$ is the local normal to the surface $\gamma = \text{const}$, the minus sign arises because the integration is done toward deeper values of z_r. The second term on the left hand side is zero because of the non-divergence of the velocity and the first term can be written as:

$$\int\limits_{V(z_r)} \frac{\partial\gamma}{\partial t} dV = \frac{\partial}{\partial t} \int\limits_{V(z_r)} \gamma_r dV' - \gamma_r \underbrace{\frac{\partial V(z_r)}{\partial t}}_{=0} \quad \text{(C4)}$$

The second term on the right hand side is zero because the total volume at constant z_r is independent of time (see formula (7)).

10   Using (C4) and the z_r derivative of (C3) we get:

$$\frac{\partial\gamma_r}{\partial t} = \frac{1}{A(z_r)}\frac{\partial}{\partial z_r}\left(A(z_r)K_{\text{eff}}(z_r)\frac{\partial\gamma_r}{\partial z_r}\right) + \text{NL} + \text{forcing} \quad \text{(C5)}$$

where we have used formula (7) and the fact that the volume integral of a z_r only function can be expressed as an integral over the reference depth:

$$\frac{\partial}{\partial z_r}\left(\frac{\partial}{\partial t}\int\limits_{V(z_r)} \gamma_r dV'\right) = \frac{\partial}{\partial t}\left(\frac{\partial}{\partial z_r}\int\limits_{z_r}^{0} A(z_r')\gamma_r(z_r',t)dz_r'\right) = -A(z_r)\frac{\partial\gamma_r}{\partial t} \quad \text{(C6)}$$

15   and with:

$$\text{NL} = \frac{1}{A(z_r)}\frac{\partial}{\partial z_r}\left(\int\limits_{V(z_r)}\left(K\nabla\theta \cdot \nabla(\frac{\partial\gamma}{\partial\theta}) + K\nabla S \cdot \nabla(\frac{\partial\gamma}{\partial S})\right)dV\right) \quad \text{(C7)}$$

and

$$\text{forcing} = -\frac{1}{A(z_r)}\frac{\partial}{\partial z_r}\left(\int\limits_{V(z_r)} f_\gamma dV\right) \quad \text{(C8)}$$

and finally K_{eff} given by formula (10).

20   *Acknowledgements.* This work was supported by the grant NE/K016083/1 "Improving simple climate models through a traceable and process-based analysis of ocean heat uptake (INSPECT)" of the UK Natural Environment Research Council (NERC). Modeling results presented in this study are available upon request to the corresponding author.

References

de Boyer Montégut, C., Madec, G., Fischer, A. S., Lazar, A., and Iudicone, D.: Mixed layer depth over the global ocean: An examination of profile data and a profile-based climatology, Journal of Geophysical Research: Oceans, 109, 2004.

Forget, G., Ferreira, D., and Liang, X.: On the observability of turbulent transport rates by Argo: supporting evidence from an inversion experiment, Ocean Science, 11, 839, 2015.

Gnanadesikan, A., Pradal, M.-A., and Abernathey, R.: Isopycnal mixing by mesoscale eddies significantly impacts oceanic anthropogenic carbon uptake, Geophysical Research Letters, 42, 4249–4255, 2015.

Gouretski, V. and Koltermann, K. P.: WOCE global hydrographic climatology, Berichte des BSH, 35, 1–52, 2004.

Griffies, S. M., Pacanowski, R. C., and Hallberg, R. W.: Spurious diapycnal mixing associated with advection in az-coordinate ocean model, Monthly Weather Review, 128, 538–564, 2000.

Hill, C., Ferreira, D., Campin, J.-M., Marshall, J., Abernathey, R., and Barrier, N.: Controlling spurious diapycnal mixing in eddy-resolving height-coordinate ocean models–Insights from virtual deliberate tracer release experiments, Ocean Modelling, 45, 14–26, 2012.

Huber, M., Tailleux, R., Ferreira, D., Kuhlbrodt, T., and Gregory, J.: A traceable physical calibration of the vertical advection-diffusion equation for modeling ocean heat uptake, Geophysical Research Letters, 42, 2333–2341, doi:10.1002/2015gl063383, <GotoISI>://WOS: 000353988700034, 0, 2015.

Ilıcak, M., Adcroft, A. J., Griffies, S. M., and Hallberg, R. W.: Spurious dianeutral mixing and the role of momentum closure, Ocean Modelling, 45, 37–58, 2012.

Iselin, C. O.: The influence of vertical and lateral turbulence on the characteristics of the waters at mid-depths, Eos, Transactions American Geophysical Union, 20, 414–417, 1939.

Jackett, D. R. and McDougall, T. J.: A neutral density variable for the world's oceans, Journal of Physical Oceanography, 27, 237–263, doi:10.1175/1520-0485(1997)027<0237:andvft>2.0.co;2, <GotoISI>://WOS:A1997WK25500002, 279, 1997.

Klocker, A. and McDougall, T. J.: Influence of the Nonlinear Equation of State on Global Estimates of Dianeutral Advection and Diffusion, Journal of Physical Oceanography, 40, 1690–1709, doi:10.1175/2010jpo4303.1, <GotoISI>://WOS:000281520800002, klocker, Andreas/E-4632-2011 Klocker, Andreas/0000-0002-2038-7922 30, 2010.

Klocker, A., McDougall, T., and Jackett, D.: A new method for forming approximately neutral surfaces, Ocean Science, 5, 155–172, 2009.

Kuhlbrodt, T. and Gregory, J.: Ocean heat uptake and its consequences for the magnitude of sea level rise and climate change, Geophysical Research Letters, 39, 2012.

Ledwell, J. R., Watson, A. J., and Law, C. S.: Mixing of a tracer in the pycnocline, Journal of Geophysical Research: Oceans, 103, 21 499– 21 529, 1998.

Lee, M.-M., Coward, A. C., and Nurser, A. G.: Spurious diapycnal mixing of the deep waters in an eddy-permitting global ocean model, Journal of Physical Oceanography, 32, 1522–1535, 2002.

Lumpkin, R. and Speer, K.: Global ocean meridional overturning, Journal of Physical Oceanography, 37, 2550–2562, 2007.

McDougall, T. J.: thermobaricity, cabbeling, and water-mass conversion, Journal of Geophysical Research-Oceans, 92, 5448–5464, doi:10.1029/JC092iC05p05448, <GotoISI>://WOS:A1987H434300036, 134, 1987.

McDougall, T. J. and Jackett, D. R.: On the helical nature of neutral trajectories in the ocean, Progress in Oceanography, 20, 153–183, doi:10.1016/0079-6611(88)90001-8, <GotoISI>://WOS:A1988T679900001, 26, 1988a.

McDougall, T. J. and Jackett, D. R.: On the helical nature of neutral trajectories in the ocean, Progress in Oceanography, 20, 153–183, 1988b.

McDougall, T. J. and Jackett, D. R.: An assessment of orthobaric density in the global ocean, Journal of Physical Oceanography, 35, 2054–2075, 2005.

McDougall, T. J., Groeskamp, S., and Griffies, S. M.: On geometrical aspects of interior ocean mixing, Journal of Physical Oceanography, 44, 2164–2175, 2014.

Megann, A.: Estimating the numerical diapycnal mixing in an eddy-permitting ocean model, Ocean Modelling, 121, 19 – 33, doi:https://doi.org/10.1016/j.ocemod.2017.11.001, http://www.sciencedirect.com/science/article/pii/S1463500317301762, 2018.

Montgomery, R.: The present evidence on the importance of lateral mixing processes in the ocean, Bulletin of the American Meteorological Society, 21, 87–94, 1940.

Munk, W. and Wunsch, C.: Abyssal recipes II: energetics of tidal and wind mixing, Deep-Sea Research Part I-Oceanographic Research Papers, 45, 1977–2010, doi:10.1016/s0967-0637(98)00070-3, <GotoISI>://WOS:000077617000001, 837, 1998.

Munk, W. H.: Abyssal recipes, in: Deep Sea Research and Oceanographic Abstracts, vol. 13, pp. 707–730, Elsevier, 1966.

Nurser, A. J. G., Marsh, R., and Williams, R. G.: Diagnosing water mass formation from air-sea fluxes and surface mixing, Journal of Physical Oceanography, 29, 1468–1487, doi:10.1175/1520-0485(1999)029<1468:dwmffa>2.0.co;2, <GotoISI>://WOS:000081739100006, marsh, Robert/G-4988-2013; Williams, Richard/0000-0002-3180-7558 66, 1999.

Polzin, K. L., Toole, J. M., Ledwell, J. R., and Schmitt, R. W.: Spatial variability of turbulent mixing in the abyssal ocean, Science, 276, 93–96, doi:10.1126/science.276.5309.93, <GotoISI>://WOS:A1997WR38600052, schmitt, Raymond /B-7451-2011 586, 1997.

Pradal, M.-A. and Gnanadesikan, A.: How does the Redi parameter for mesoscale mixing impact global climate in an Earth system model?, Journal of Advances in Modeling Earth Systems, 6, 586–601, 2014.

Redi, M. H.: Oceanic isopycnal mixing by coordinate rotation, Journal of Physical Oceanography, 12, 1154–1158, 1982.

Saenz, J. A., Tailleux, R., Butler, E. D., Hughes, G. O., and Oliver, K. I. C.: Estimating Lorenz's Reference State in an Ocean with a Nonlinear Equation of State for Seawater, Journal of Physical Oceanography, 45, 1242–1257, doi:10.1175/jpo-d-14-0105.1, <GotoISI>://WOS:000354370700003, 1, 2015.

Solomon, H.: On the representation of isentropic mixing in ocean circulation models, Journal of Physical Oceanography, 1, 233–234, 1971.

Speer, K. G.: A note on average cross-isopycnal mixing in the North Atlantic ocean, Deep-Sea Research Part I-Oceanographic Research Papers, 44, 1981–1990, doi:10.1016/s0967-0637(97)00054-x, <GotoISI>://WOS:000072760700004, speer, KG, 1997.

Tailleux, R.: Neutrality Versus Materiality: A Thermodynamic Theory of Neutral Surfaces, Fluids, 1, 32, 2016.

Urakawa, L., Saenz, J., and Hogg, A.: Available potential energy gain from mixing due to the nonlinearity of the equation of state in a global ocean model, Geophysical Research Letters, 40, 2224–2228, 2013.

Walin, G.: on the relation between sea-surface heat flow and thermal circulation in the ocean, Tellus, 34, 187–195, <GotoISI>://WOS:A1982NJ88300010, 180, 1982.

Winters, K. B. and D'Asaro, E. A.: Diascalar flux and the rate of fluid mixing, Journal of Fluid Mechanics, 317, 179–193, 1996.